Available online at www.sciencedirect.com
ScienceDirect
International Communications in Heat and Mass Transfer 33 (2006) 1088–1095
International Communications in HEAT and MASS TRANSFER
www.elsevier.com/locate/ichmt

Measurement of mixing of two miscible liquids in a stirred vessel with electrical resistance tomography ☆

Sin Kim [a,*], Andre Ngansib Nkaya [b], Tomasz Dyakowski [b]

[a] Department of Nuclear and Energy Engineering, Cheju National University, Cheju 690 756, Korea
[b] School of Chemical Engineering and Analytical Science, University of Manchester, Manchester M60 1QD, United Kingdom

Available online 12 July 2006

Abstract

An electrical resistance tomography (ERT) system is used to measure the mixing of two miscible liquids. A data analysis method to monitor and measure the mixing process is proposed. On the basis of the reconstructed pixel conductivity data obtained from multi-plane ERT sensors, the mixing time can be measured and the best-correlated pairs of pixels are identified to determine the dispersion velocity of the secondary liquid in the primary liquid as well. Experimental results for the mixing of liquids in a stirred tank are presented.

Keywords: Mixing; Miscible liquids; Electrical resistance tomography; Process tomography

1. Introduction

Mixing is a common process in many industrial applications, but due to its complexity theoretical approaches are very limited. Monitoring or measuring the mixing properly is of great importance from the practical point of view and for the validation of theoretical models as well. In this work, the electrical resistance tomography (ERT) technique has been adopted to obtain the mixture distribution across the cross-section of the mixing vessel. The ERT has attracted many researchers' interests in the field of the process tomography because of its obvious advantages including non-intrusive measurement, high temporal resolution and non-radiological characteristics [1]. In ERT, different current patterns are applied to the flow field through electrodes attached on the boundary and the corresponding voltages are measured. Based on the current–voltage relation, the internal electrical conductivity distribution, that is the mixture concentration distribution, is estimated. In general, the estimated conductivity distribution is expressed as pixel images that provide instantaneous information on a concentration distribution in a flow domain at a given location.

☆ Communicated by W.J. Minkowycz.

* Corresponding author. Tel.: +82 64 754 3647; fax: +82 64 757 9276.
E-mail address: sinkim@cheju.ac.kr (S. Kim).

0735-1933/$ - see front matter © 2006 Elsevier Ltd. All rights reserved.
doi:10.1016/j.icheatmasstransfer.2006.06.010

Nomenclature

C	Relative conductivity
C_m	Cross-sectional average of C
D	Relative deviation of C
R	Cross-correlation function
$\tilde{R}$	Best-correlated cross-correlation function
S	Cross-sectional standard deviation of c
t_{95}, t_{99}	Mixing time to reach $D<0.05$ and $D<0.01$, respectively
ρ	Best-correlated cross-correlation coefficient

The electrical impedance imaging technique including ERT and ECT (electrical capacitance tomography) has been applied to the process tomography of mixture fields. Using ERT, macromixing of miscible liquids in a stirred vessel was imaged and the different mixing patterns from two types of impeller in 3-D was successfully distinguished [2]. Gas–liquid mixing in a stirred vessel was measured with ERT and the effect of the liquid viscosity on mixing behaviour was investigated [3]. ECT also has been widely applied to the visualisation of various multi-phase flows for the industrial and research purposes [4]. In addition, the images were analysed to track dispersion, stretch and rotation of the concentration distribution and to investigate the uniformity [5]. For fluid–solid mixtures, the solid velocity and mass flow rate were measured with cross-correlation techniques [6,7]. This paper aims at the application of ERT to visualise and analyse the mixing of two miscible liquids in a stirred vessel where miscible liquids have distinct conductivities.

Using multi-layered 16-electrode arrays, multi-layered tomograms are reconstructed. The tomograms, namely the cross-sectional mixture distributions, at the predetermined elevations are instantaneously visualised as pixel images. The application of ERT or ECT to the visualisation of mixing is not new as can be seen in the review mentioned above. In addition to the visualisation of mixing, therefore, this work proposes a method to measure the mixing time and the dispersion velocity in the mixing of two miscible liquids. From the time evolution and the spatial distribution of pixel-based conductivity, the mixing time is measured. A cross-correlation coefficient method is introduced to find the best-correlated pixels that determine the dispersion velocity of the secondary fluid in the primary fluid.

2. ERT system

A cylindrical stirred vessel fitted with a six-bladed Rushton turbine impeller is used for mixing experiments. The diameter is 0.61 m and the height is 1.5 m. On the vessel wall, 8 planes of 16-sensor rings are mounted, but only upper 4 planes were used in this work to increase the temporal resolution. The vertical distance between neighbouring electrodes is 8.0 cm.

The current injection, voltage measurements and image reconstruction were performed with P2000 Electrical Resistance Tomography System of Industrial Process Tomography Ltd. As a current injection protocol, the adjacent pattern is used at 9.6 kHz. Conductivity distribution was reconstructed by linear back projection. The tomogram is basically presented as a square grid with $20\times20=400$ pixels. However, some of these pixels lie outside the vessel circumference and the image should be formed from the pixels inside the vessel. The circular image is therefore constructed using 316 pixels from the 400 pixel square grid. Before adding the secondary liquid to the vessel, the referenced state was measured to eliminate the effects of the stirrer and other internal structures. In other words, the change in the conductivity distribution is estimated with the change in the boundaryvoltages from the referenced ones.

3. Tomograms of mixing of two miscible liquids

The vessel was filled with tap water (primary liquid) swirled by the impeller at the rate of 150 rpm. The data collection and the image reconstruction were made online and the temporal resolution was 1.44 s/frame. At about

40 frames after the initiation of the measurement, 200 ml brine of concentration 10 g/l (secondary liquid) is added to the water volume. The measurements were continued for 250 frames, which were long enough for the mixture to be sufficiently homogenised. Fig. 1 shows the tomograms of the relative conductivity σ/σ_0 at the selected frames. In this, σ and σ_0 denote the conductivity of the mixture and the conductivity of the primary liquid. The planes are designated as P1, P2, P3 and P4 in turn from the top. Upon adding brine to tap water, the tomogram at the top plane (P1) immediately indicates the change in the conductivity distribution at the centre region. The darkness represents the relative conductivity. Then, the black spot becomes larger and thicker while the addition of brine continues for about 20 s. Also, it penetrates down to P2, P3 and P4 planes in order. Passing about the 55th frame, the darkness at P1 turns into lighter. At lower planes, however, the black spots continue to get darker for a

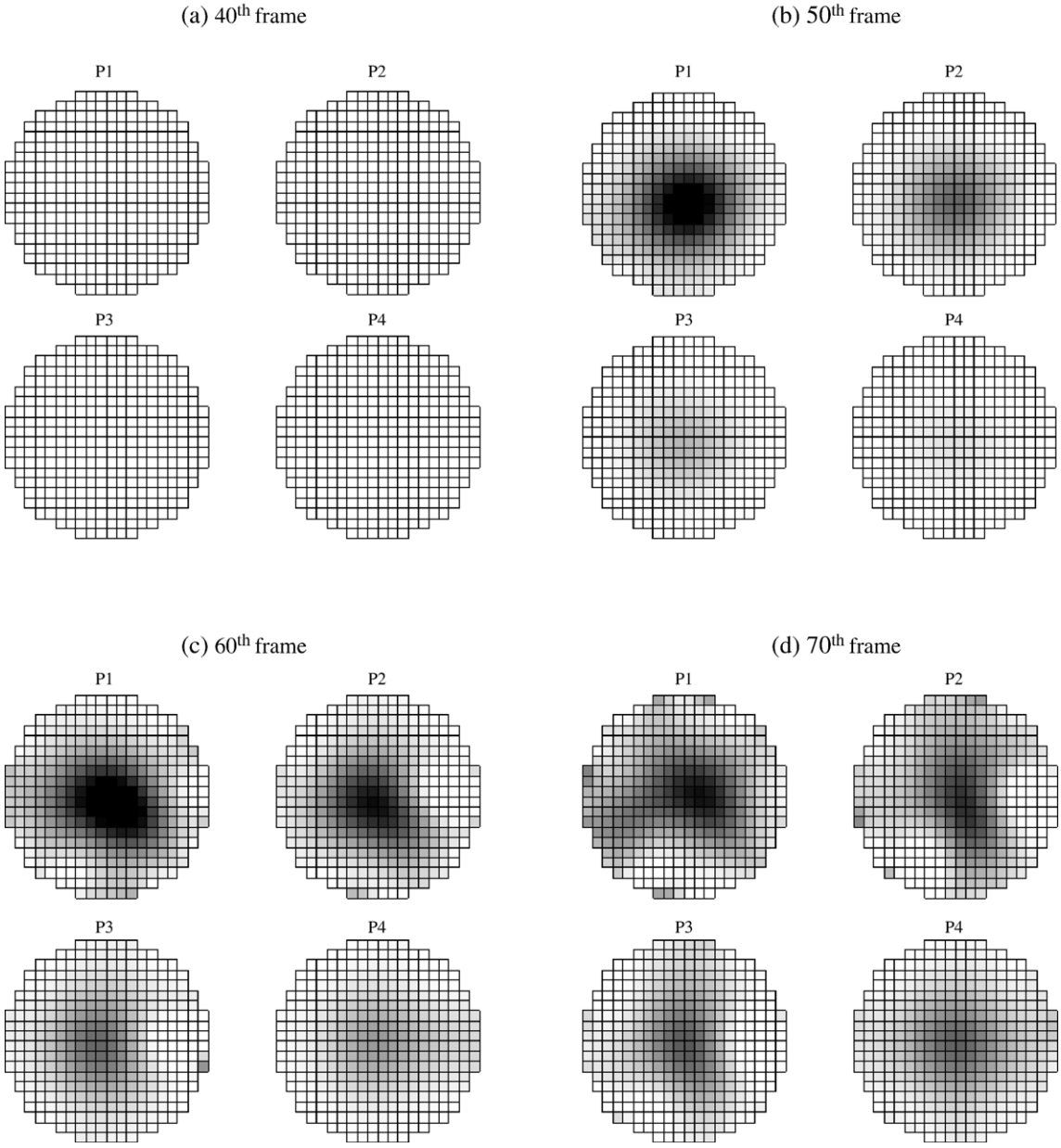

Fig. 1. Tomograms of relative conductivity. (a) 40th frame, (b) 50th frame, (c) 60th frame, (d) 70th frame, (e) 80th frame, (f) 90th frame, (g) 100th frame, (h) 110th frame.

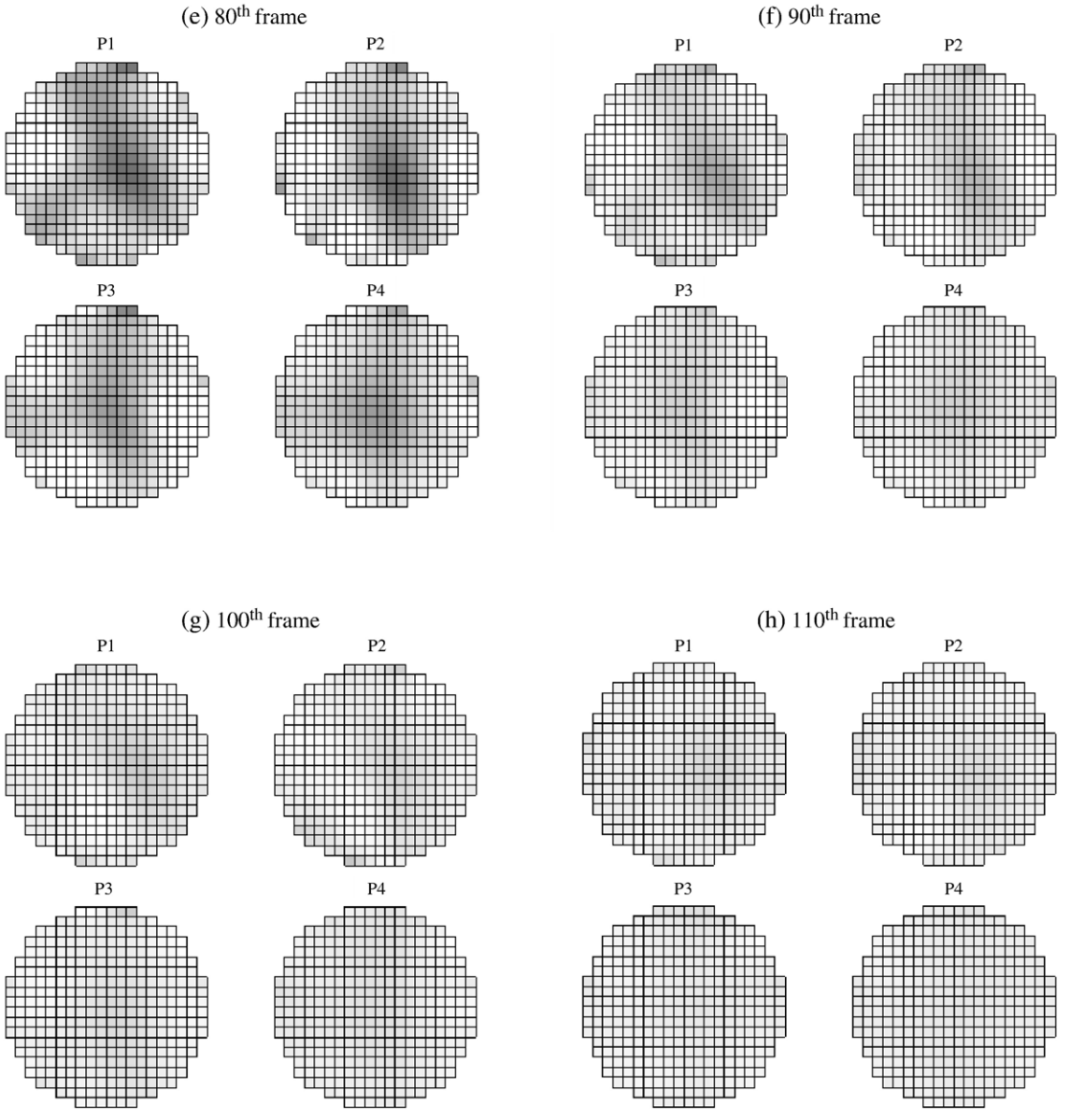

Fig. 1 (*continued*).

while. After the 80th frame, all spots become blurred. With the above observation of the tomograms in time sequence, qualitative features during the mixing of two miscible liquids could be grasped. From practical and theoretical points of view, however, the quantitative information on the mixing would be more desirable. Thus, a pixel-based analysis is introduced.

4. Mixing time

Let us denote the relative conductivity of the kth pixel at the jth frame in the ith plane as $C[i,j,k]$, $i=1,\cdots,N_{\mathrm{pl}}$, $j=1,\cdots,N_{\mathrm{fr}}$, and $k=1,\cdots,N_{\mathrm{px}}$. In this, N_{pl}, N_{fr} and N_{px} are the number of planes, frames and pixels, respectively. In the present work, $N_{\mathrm{pl}}=4$, $N_{\mathrm{fr}}=250$ and $N_{\mathrm{px}}=316$.

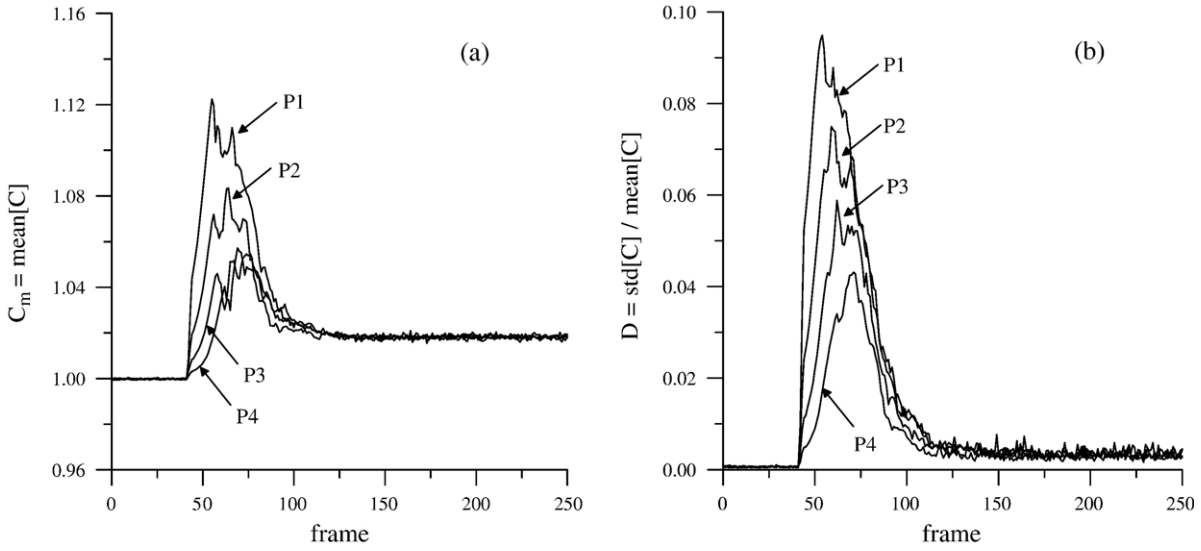

Fig. 2. Cross-sectional average (a) and relative deviation (b).

At first, let us find the times at which the addition of brine starts and ends. Fig. 2 shows the time evolution of $C_m[i,j,\bullet]$ and $D[i,j]$ where $C_m[i,j,\bullet]$ is the cross-sectional average of $C[i,j,k]$ and the relative deviation $D[i,j]$ is defined as

$$D[i,j] = \frac{S[i,j,\bullet]}{C_m[i,j,\bullet]} \tag{1}$$

In this, $S[i,j,\bullet]$ is the cross-sectional standard deviation of $C[i,j,k]$. The dot means that the operation is done on that index location. As can be seen in Fig. 2, initially, $C_m[i,j,\bullet]$ is virtually unity and $D[i,j]$ is nearly zero because the vessel is filled with tap water only. However, $D[i,j]$ becomes to depart from zero past around the 40th frame, which may corresponds to the instance of brine addition. Up to the 41st frame, $D[i,j]$'s for all planes remain less than 0.001. At the 42nd frame, $D[i,j]$ starts to increase suddenly by at least two times. Thus, it is concluded that the addition of brine starts at the 42nd frame. It should be noted that the brine lump does not reach all planes at the same time although the frame numbers when $D[i,j]>0.001$ are same for all plane. In fact, the electrical field in the vessel is three-dimensional. Even before reaching a plane the brine lump may affect the reconstructed conductivity distribution at the plane. The frame at which the maximum of $C_m[i,j,\bullet]$ for P1 is found may be the end frame of brine addition and it is the 55th frame. Hence, the addition of brine has been continued for 13 frames.

The mixing time may be one of the major parameters in mixing analysis. The mixing time is the time taken for the concentration distribution at a plane to reach or nearly reach a uniform distribution or the expected final mean concentration after the addition of the secondary fluid. In practice, the uniform distribution could never been reached due to measurement noise and the final mean concentration would be unknown. Thus, in this work, the mixing time is taken as the time at which the relative deviation $D[i,j]$ decreases below the predetermined small value m.

$$D[i,j] < m \tag{2}$$

In most cases, t_{95} or t_{99} is measured, i.e. the time from the addition of the secondary liquid to the time when $m=0.05$ or 0.01. The frame number at which $D[i,j]>0.01$ is 109 for P1, 106 for P2, 98 for P3 and 91 for P4. Therefore, the mixing time measured from the end of brine addition is obtained as $t_{99}=77.8$ s, 73.4 s, 61.9 s and 51.8 s for P1, P2, P3 and P4, respectively. As expected, the mixing time decreases as the distance from the top since the concentration of brine dilutes as it passes down.

5. Cross-correlation and dispersion velocity

A cross-correlation technique has been applied for measuring solid velocity in gas–solid flows [6,7]. In this technique, multiple sensors placed along the flow stream are used. If a signal is detected in the upstream sensor and

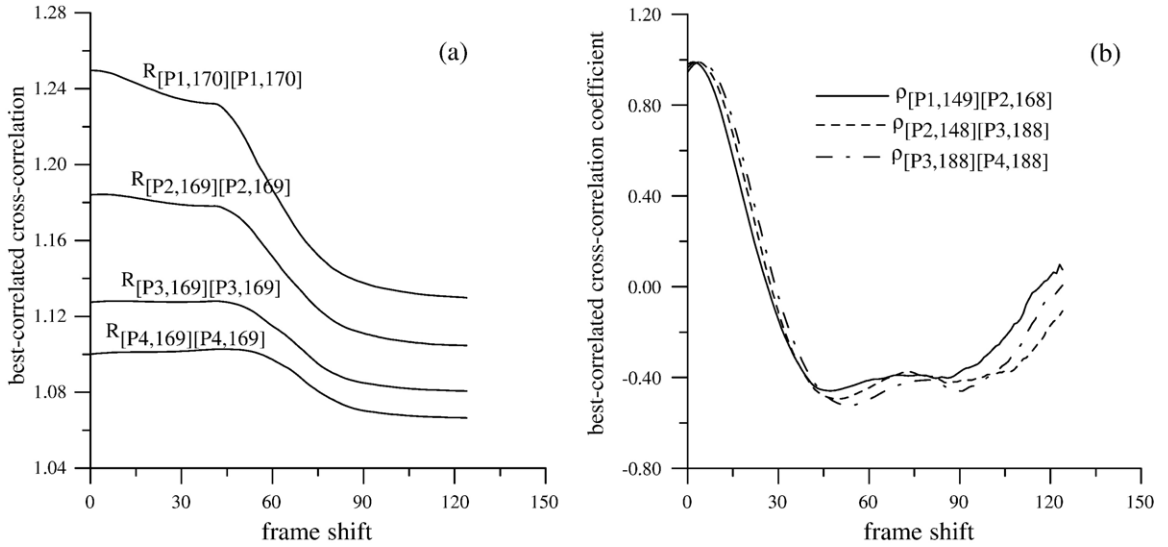

Fig. 3. Best-correlated cross-correlation (a) and cross-correlation coefficient (b).

reappears at the downstream sensor and if the time interval ΔT between the detections and the distance L between the two sensors are known, then the velocity V can be calculated as

$$V = L/\Delta T. \tag{3}$$

In reality, signals from actual flows will change between the two sensors due to flow turbulence and varying mixture distribution. Hence, a cross-correlation should be introduced to find the most similar signal pairs. A cross-correlation function is defined as

$$R_{F[X],F[Y]}(\tau) = \lim_{T\to\infty} \frac{1}{T}\int_0^T F_X(t)F_Y(t+\tau)\mathrm{d}t\,. \tag{4}$$

where F_X and F_Y are the detected signals from the sensor X and Y, respectively. τ is a time delay and T is a time period for which the cross-correlation is calculated. The correlation function reaches the maximum at time delay τ_{max}, which is an estimate of the transit time of the object between two sensors. Since tomograms from ERT technique are obtained

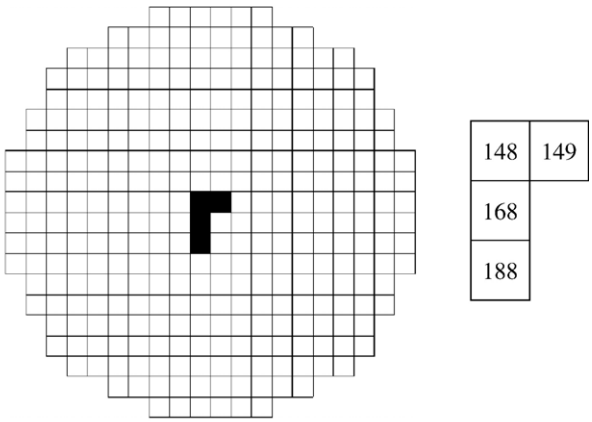

Fig. 4. Pixels for the best-correlated cross-correlation coefficient pairs.

as pixel-based images and the conductivity is measured discretely in the temporal coordinate, the cross-correlation function can be calculated as [6]

$$R_{F[X,\bullet,m],F[Y,\bullet,n]}[p] = \frac{1}{N}\sum_{j=1}^{N} F[X,j,m]F[Y,j+p,n],\ \ m,n \in B\,. \tag{5}$$

where $F[X,j,m]$ stands for the signal of the pixel m at the frame j in the plane X, p is the shift number in time sequence of frames, N is the number of samples in the summation and B is the region of interest. Among $R_{F[X,\bullet,m],F[Y,\bullet,n]}[p]$, the best-correlated pixel pair (m,n) is chosen. Set the best-correlated cross-correlation function to be $\tilde{R}_{F[X,\cdot,m],F[Y,\cdot,n]}[p]$. From this pair, the peak shift $p_{\max}$, which gives the maximum value of the cross-correlation function between the pixel m of the plane X and the pixel n of the plane Y, can be calculated.

The best-correlated auto-correlation function for each plane $\tilde{R}_{C[X,\cdot,m],C[X,\cdot,n]}[p]$ is given in Fig. 3(a). For simplicity, '∼', C and the dot are dropped in the figure. The peak shifts $p_{\max}$ for P1, P2, P3 and P4 are found at 1, 4, 10 and 43, respectively. It seems to be irrational that the peak shift for the auto-correlation is not zero. This unreasonable result is caused by the fact that the initial and the final conductivity are nearly constant but not same with each other. Hence, it would be better to employ the cross-correlation coefficient rather than the cross-correlation function. The best-correlated cross-correlation coefficient is defined as

$$\rho_{C[X,\bullet,m],F[Y,\bullet,n]}[p] = \frac{\mathrm{cov}(C[X,\bullet,m], C[Y,\bullet,n])}{S[X,\bullet,m]S[Y,\bullet,n]}\,, \tag{6}$$

where (m,n) is the best-correlated pair. The best-correlated cross-correlation coefficients between neighbouring two planes are plotted in Fig. 3(b). Again, for simplicity, C and the dot are dropped in the figure. Now, the peak shift is found to be 0 for all the auto-correlation coefficients. The peak shift for neighbouring two planes is 2 for (P1,P2), 3 for (P2,P3) and 4 for (P3,P4). The pixel indices for the best-correlated cross-correlation coefficient pairs are (149,168) for (P1,P2), (148,188) for (P2,P3) and (188,188) for (P3,P4). These pixels are marked in Fig. 4. The peak shift for neighbouring two planes tends to increase as the brine lump penetrates down to the bottom. The dispersion speeds are calculated as 3.1 cm/s for P1→P2, 2.3 cm/s for P2→P3 and 1.4 cm/s for P3→P4.

6. Conclusions

The mixing of two miscible liquids in a vessel with a rotating agitator has been measured with a four-plane electrical resistance tomography system. The mixing process was monitored online with the aid of the reconstructed conductivity distribution. The pixel-based images were successfully used to determine the mixing time and the dispersion velocity of the secondary liquid in the primary liquid. The mixing time could be calculated from the temporal trend of cross-sectional conductivity distribution. The dispersion velocity was obtained from the cross-correlation coefficient of the best-correlated pixels between two adjacent planes since the cross-correlation function, which has been commonly adopted for solid velocity measurements in solid–gas flows, might give unrealistic results of non-zero peak shifts even for the auto-correlation. The presented data analysis method with ERT will be useful to measure and analyse the mixing in the process tomography.

Acknowledgements

This work was supported by the Korea Research Foundation Grant (KRF-2005-013-D00075).

References

[1] M.S. Beck, R.A. Williams, Process tomography: a European innovation and its applications, Measurement Science and Technology 7 (3) (1996) 215–224.
[2] P.J. Holden, M. Wang, R. Mann, F.J. Dickin, R.B. Edwards, Imaging stirred-vessel macromixing using electrical resistance tomography, AIChE Journal 44 (4) (1998) 780–790.
[3] M. Wang, A. Dorward, D. Vlaev, R. Mann, Measurements of gas–liquid mixing in a stirred vessel using electrical resistance tomography (ERT), Chemical Engineering Journal 77 (1–2) (2000) 93–98.

[4] N. Reinecke, D. Mewes, Recent developments and industrial/research applications of capacitance tomography, Measurement Science and Technology 7 (3) (1996) 233–246.
[5] L. Li, J. Wei, Three-dimensional image analysis of mixing in stirred vessels, AIChE Journal 45 (9) (1999) 1855–1865.
[6] V. Mosorov, D. Sankowski, L. Mazurkiewicz, T. Dyakowski, The 'best-correlated pixels' method for solid mass flow measurements using electrical capacitance tomography, Measurement Science and Technology 13 (12) (2002) 1810–1814.
[7] S. Liu, Q. Chen, H.G. Wang, F. Jiang, I. Ismail, W.Q. Yang, Electrical capacitance tomography for gas–solids flow measurement for circulating fluidized beds, Flow Measurement and Instrumentation 16 (2–3) (2005) 135–144.